STUDY OF ELECTRICAL CHARACTERISTIC OF TRANSVERSE ARC ARRAY DISCHAGE IN GASES

Teh, M. T.[1], Low, K. S.[2]

[1]Physics with Electronics Programme, School of Science and Technology,
Universiti Malaysia Sabah, Locked Bag 2073, 88999 Kota Kinabalu, Sabah.

[2]Laser and Photonic Laboratory, University of Malaya,
50603 Lembah Pantai, Kuala Lumpur.

ABSTRACT. *A table-top soft x-ray laser operating at 46.9 nm with a pulse energy of 1 mJ has been demonstrated by Rocca J. J. (Rocca, 1999) using capillary discharge scheme. However, it is difficult to scale up in length due to excessively high voltages required. In this study, the alternative discharge scheme of transverse arc array examined previously is further investigated here. In the alternatively discharge scheme, an array of electrodes are placed side by side and discharged transversely to the optical axis. By charging separately sets of capacitors and then discharging separately into the electrodes, an array of arc discharges is produced. Each electrode can be considered to constitute approximately a capillary discharge. Scaling of power involves simply by increasing the number of electrodes in the array. Different electrode configurations have been applied to investigate the ability of the electrodes to hold higher voltages before breakdown. Two gases have been used as the active media i.e. nitrogen and argon. The electrical characteristic of this arc array discharge scheme has to be studied in detail before it can be scaled up to pump short wavelength lasers.*

Keywords: transverse arc array,capillary discharge, short wavelength lasers.

INTRODUCTION

A new transverse arc array discharge scheme has been developed as an alternative way of pumping short wavelength lasers. This transverse excitation scheme allows lower voltage driving requirement but still able to produce discharge conditions as in the capillary discharge. Previous studies *(Goh, K. S., 2000) (Ng, K. F., 2000)* had successfully demonstrated laser output at 337.1 nm with an optical output of about 1.7 mJ, using the new scheme. In that study, investigation of the laser action of the transverse arc array discharge in nitrogen gas has been carried out. In this study, the electrical characteristic of the discharge scheme in nitrogen gas is being further investigated. Study on argon gas is being carried out too since argon gas might also have chance to lase at short wavelengths. Various electrode profiles are also investigated to compare the discharge characteristics.

METHODOLOGY

The discharge system carried out in this experiment is essentially that of a pulsed gas laser except for the new electrical circuitry. It consists of various components of a fast-pulsed discharged gas laser (Shipman, J. D.,1967). The discharge system comprises of:

(1) Discharge channel
(2) Vacuum system
(3) Spark gap
(4) Storage capacitors
(5) Peaking capacitors
(6) High voltage power supply
(7) Pulsed triggering unit

In this experiment, both the storage and peaking capacitors are assembled using doorknob capacitors. A discharge system such that the electrodes are an array of individual pins, which are connected to its own set of excitation circuit is developed here. Therefore, there will be a high current to the pins, which formed arc discharge. Each set of the pin electrodes are decoupled from the rest electrically. There are 12 doorknob ceramic capacitors (0.44 nF), which act as the peaking capacitors, are screwed onto this base plate. Also, another 12 doorknob capacitors (0.7 nF) are stacked up against the peaking capacitors, which act as the storage capacitors. These form the configuration of the 'c-to-c' circuit (Fig. 1).

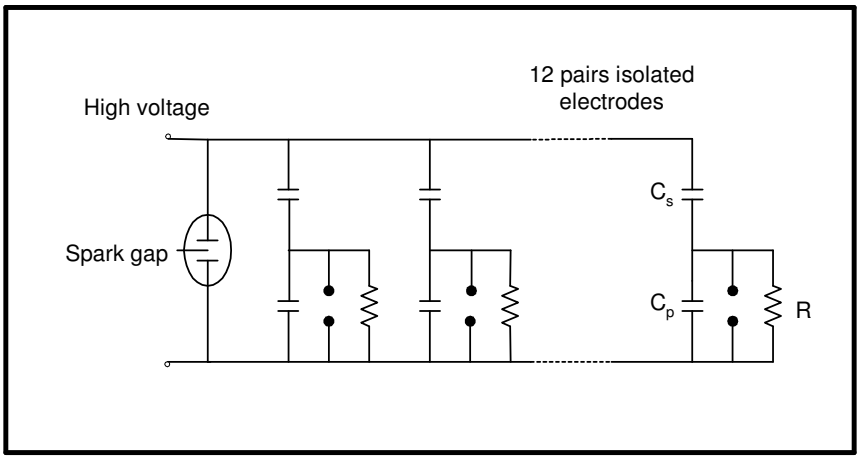

Figure 1: Schematic diagram of the extended 'c-to-c' circuit in transverse arc array discharge scheme.

In order to study the effects of the different electrode profiles for the discharge, different electrode configurations have been investigated. Hereby, three different sets of electrode configurations were employed to compare their discharge voltages at different charging voltages and operating pressures. Three sets of different electrode configurations are listed in Table 1 and show in Fig. 2. The discharge gap between the anode and cathode is fixed to be 10 mm.

Table 1: Three sets of electrode configurations employed in the experiment.

Set	Anode	Cathode
A	Round surface electrode	Cylindrical rod
B	Round surface electrode	Flat surface electrode
C	Flat surface electrode	Flat surface electrode

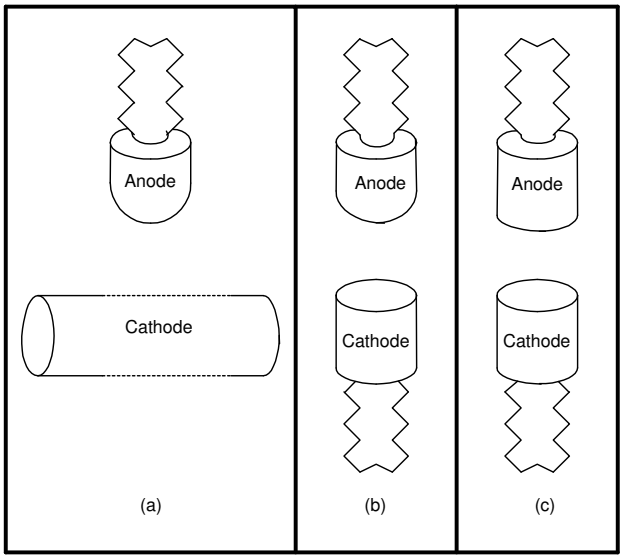

Figure 2: Three sets of the electrode configuration.

Diagnostic Devices

A digital phosphor oscilloscope (Tektronix TDS 3032) is used to obtain the discharge waveforms. The voltage measurement was taken using the high voltage probes with 1000X attenuation. The voltage probes are placed with the tips touching the point of measurement directly, without any connection to extra wires or cables in order to avoid the reception of unnecessary noise and delay. For the current measurement, a calibrated RC integrated Rogowski coil has been used.

RESULTS AND DISCUSSION

(A.) Comparison of the electrode configurations

The discharge voltage for different electrode configurations is compared for both nitrogen and argon gases. Since both gases give a very similar result, result for nitrogen gas is chosen to be discussed here. Shown below are the graphs for discharge voltage versus pressure when nitrogen gas is applied.

(I.) Set A: Round pin – to – cylindrical rod

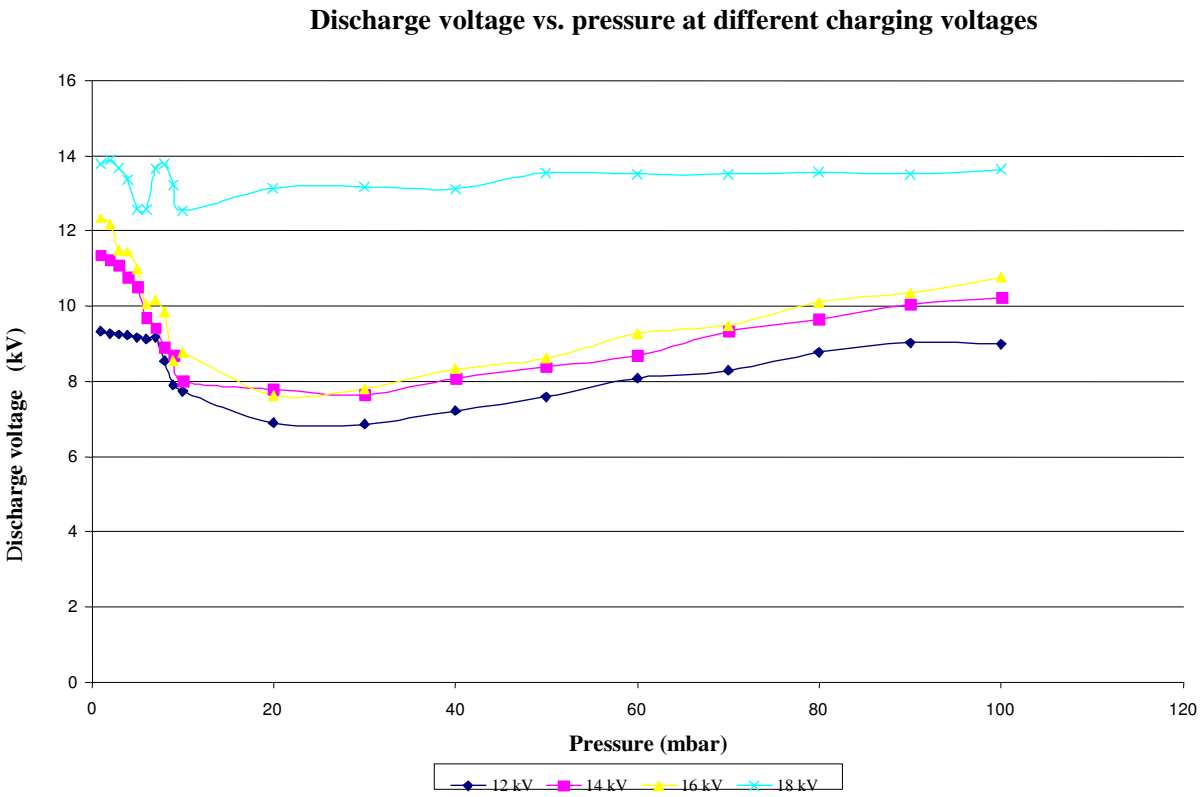

Figure 3: Discharge voltage versus pressure of electrode configuration set A at different charging voltages.

(II.) Set B: Round pin – to – flat pin

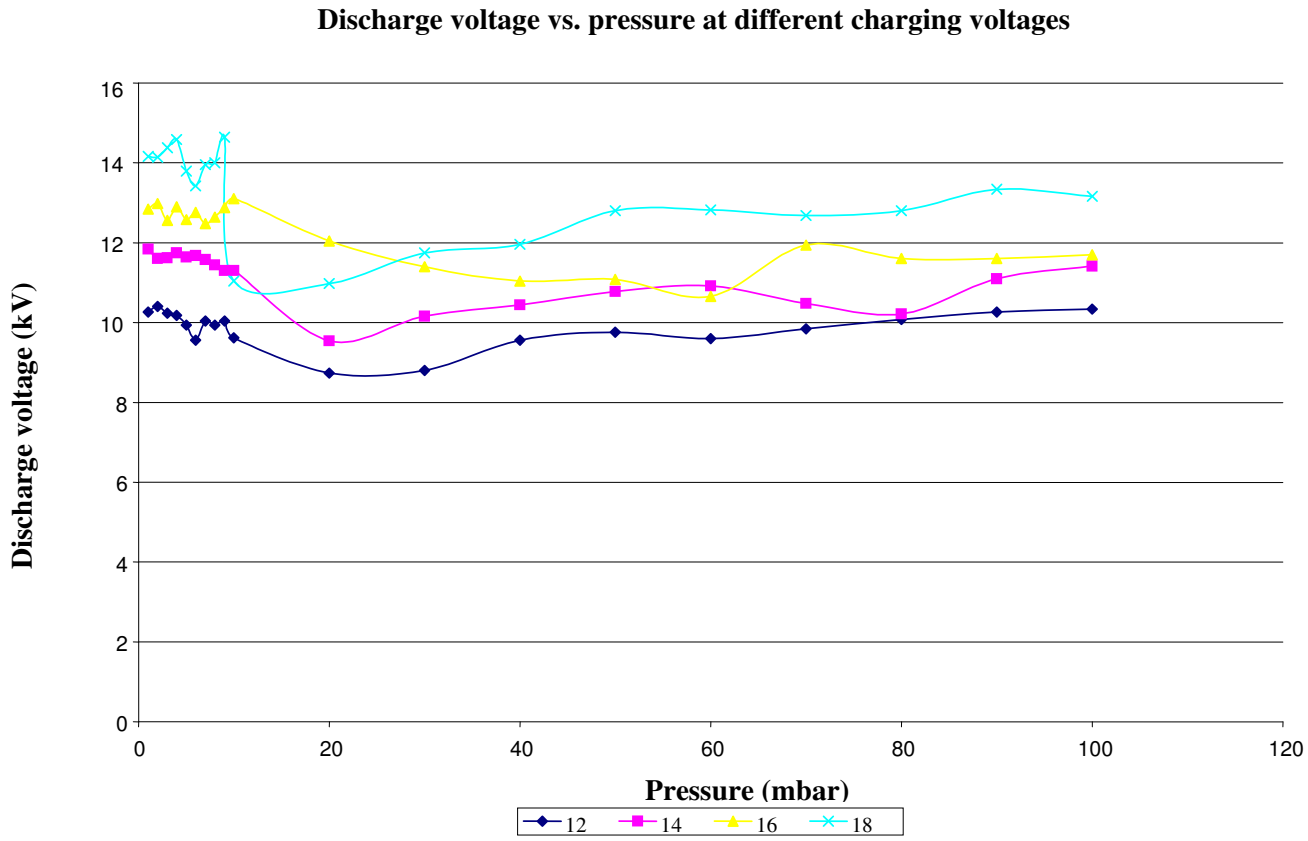

Figure 4: Discharge voltage versus pressure of electrode configuration set B at different charging voltages.

(III.) Set C: Flat pin – to – flat pin

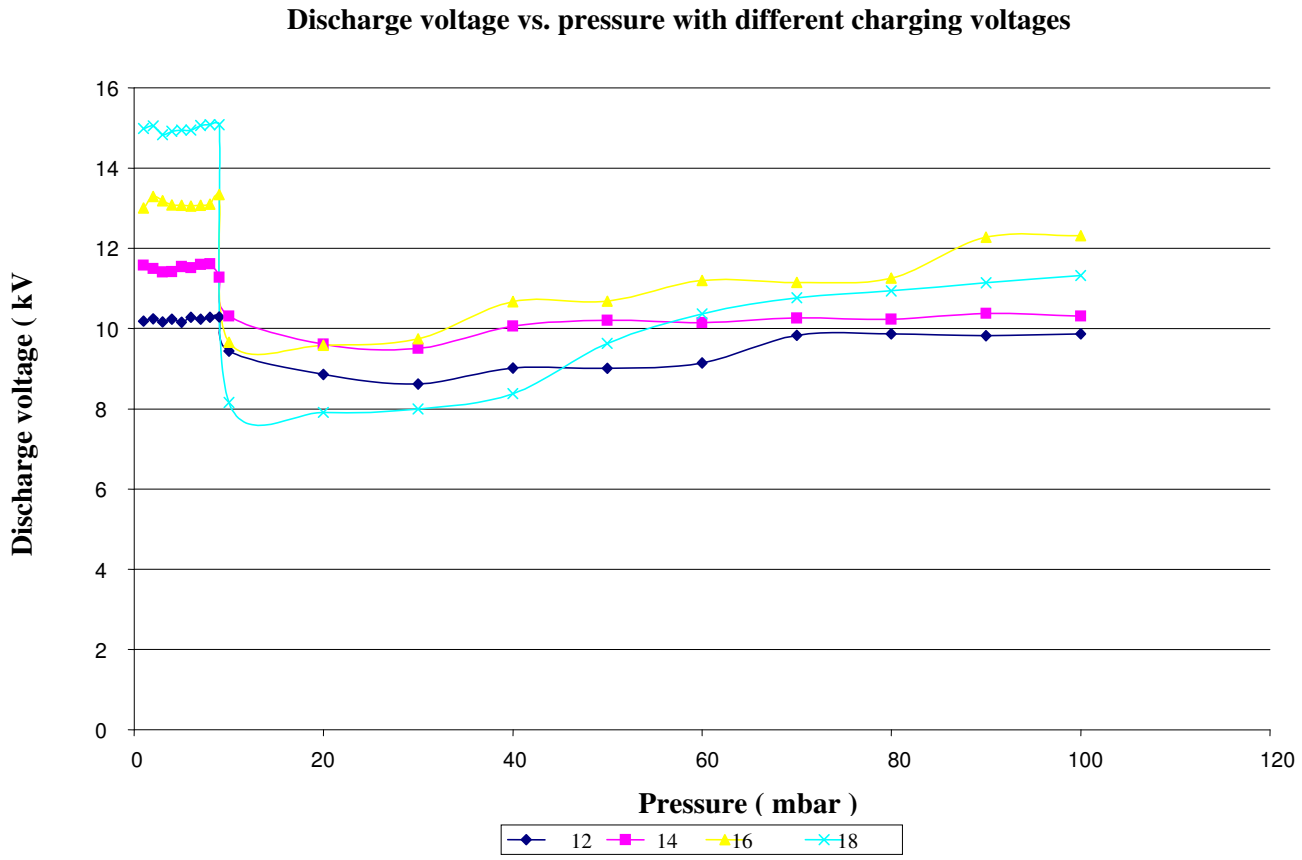

Figure 5: Discharge voltage versus pressure of electrode configuration set C at different charging voltages.

From the graphs plotted (Figure 3 – Figure 5), there is a general trend for the discharge voltage. As the pressure reduces from 100 mbar to 10 mbar, the discharge voltage reduces as well. But, when the pressure is reduced from 10 mbar to 9 mbar, the discharge voltage increases drastically. Initially, there is a minimum discharge voltage at a certain pressure, i.e. at 10 mbar. The discharge voltage starts to increase after the pressure is decreased beyond this range. The graphs also reveal that the discharge voltage increases with the charging voltage. In this experiment, the charging voltages are ranged from 12 kV to 18 kV. From this result, it shows clearly that the highest discharge voltage happens at lower pressure, i.e. $p \leq 9$ mbar. The difference is just the value of the discharge voltage measured when electrode Set C is applied is the highest among these 3 sets of electrode configurations.

(B.) Comparison of the gas mediums

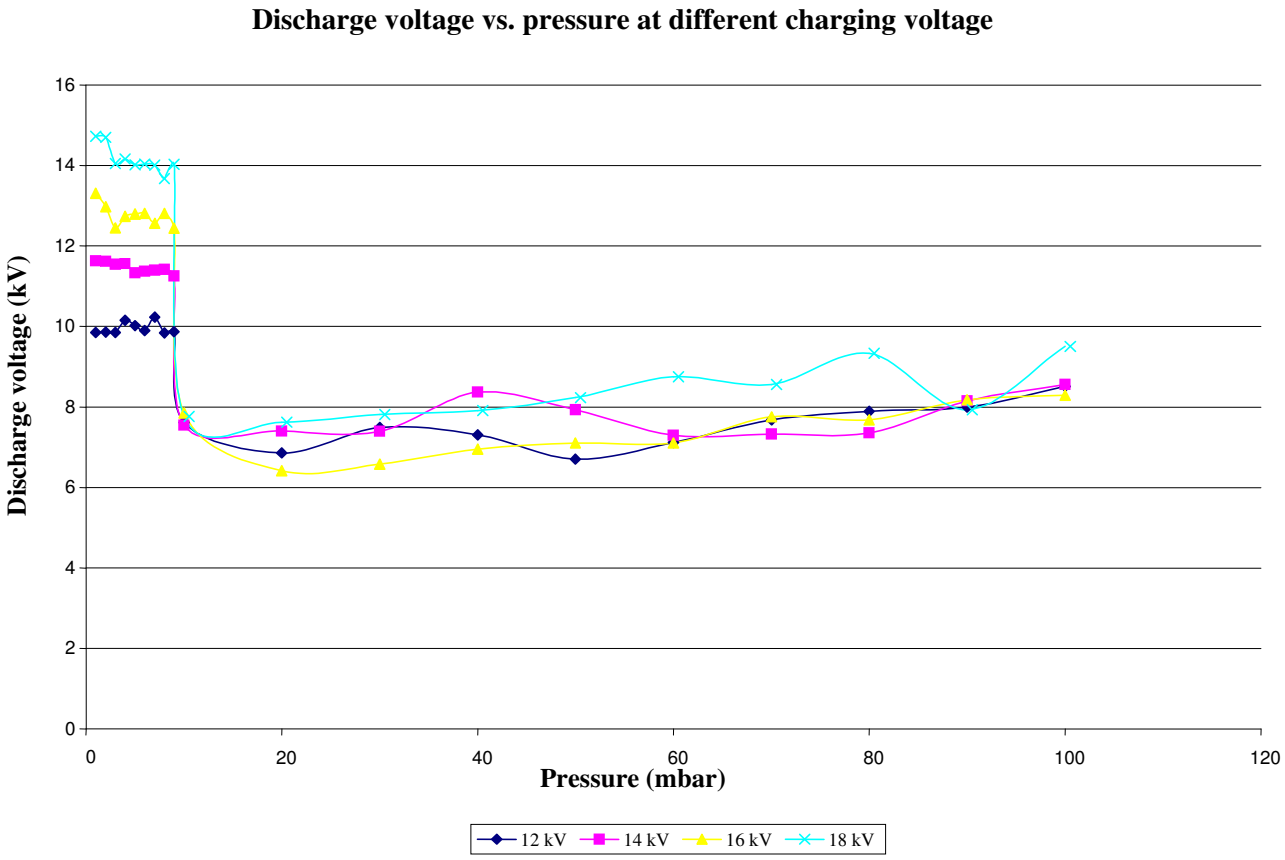

Figure 6: Discharge voltage versus pressure of electrode configuration set C at different charging voltages (argon as the active medium).

From the experimental results, both gases seemed to give very similar results (Figure 5 and Figure 6). Both shapes of the graph of discharge voltage versus pressure shows the same trend as the experiment using nitrogen or argon as the gas medium. The discharge voltage increases drastically at the pressure 9 mbar for both gases. The discharge voltage is increasing by applying different electrode configurations from Set A to C. Hence, the discharge voltage of (Set A) < (Set B) < (Set C).

(C.) Voltage and current measurements with electrode configuration of set C applied

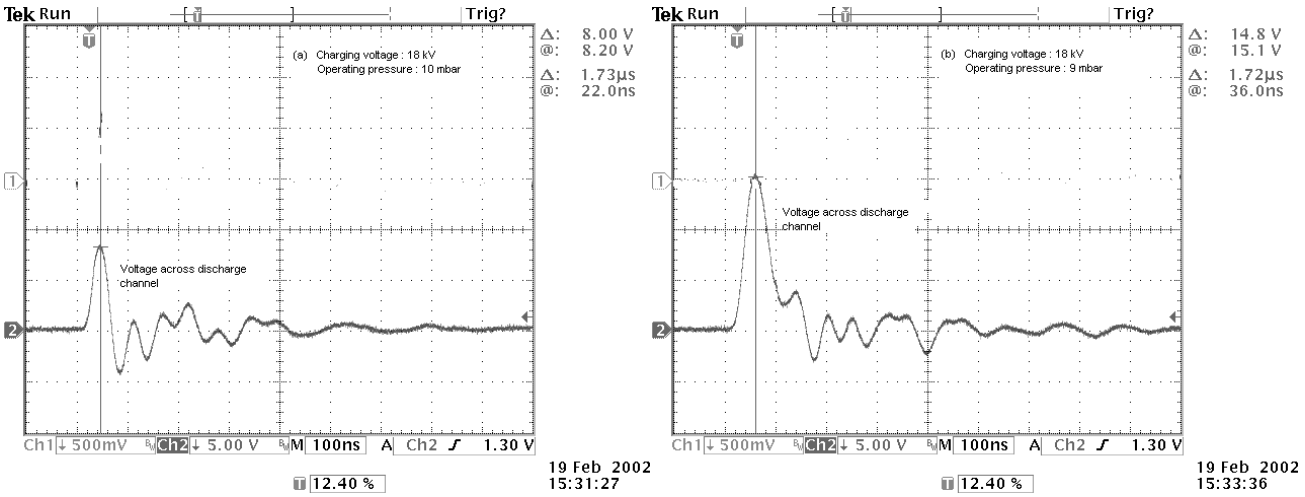

Figure 7: The discharge voltage waveform across the discharge channel at the operating pressure of (a) 10 mbar [left figure], and (b) 9 mbar [right figure] with the charging voltage of 18 kV.

Figure 7(b) shows the drastically increased discharge voltage across the discharge channel when the operating pressure was varied. The discharge voltage increases from (8.0 ± 0.1) kV to (14.8 ± 0.1) kV when the operating pressure increased from 9 mbar to 10 mbar, with the charging voltage of 18 kV. From these figures, one can conclude that the breakdown voltage is getting higher when a lower operating pressure ($p \leq 9$ mbar) is applied.

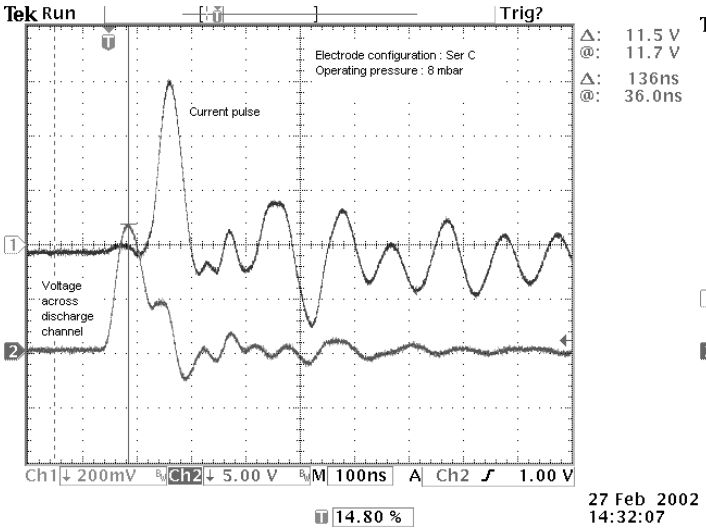

Figure 8: Current pulse measured with Rogowski coil (Chn 1) and voltage measured across discharge channel (Chn 2) operated at 8 mbar.

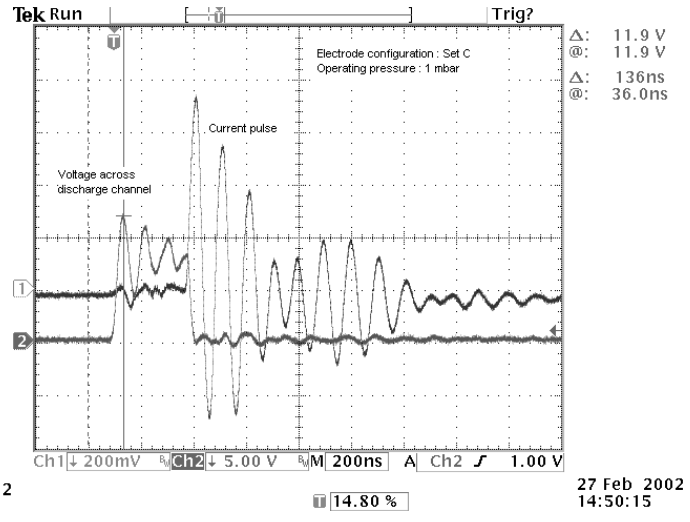

Figure 9: Current pulse measured with Rogowski coil (Chn 1) and voltage measured across discharge channel (Chn 2) operated at 1 mbar.

Fig. 8 and Fig. 9 show the voltage and current waveforms when the system is operated in 8 mbar and 1 mbar respectively. The peak current in Fig. 9 is only (100 ± 2) A, and occurs at (80 ± 10) ns after the discharge channel breakdown. As the operating pressure has been decreased to 1 mbar, the peak current achieved is (108 ± 2) A, yet it occurs at (280 ± 40) ns after the discharge channel breakdown. Both current pulse width for FWHM (Full Wave Half Maximum) of Fig. 8 and Fig. 9 are (40 ± 10) ns.

From Figure 9, we can notice that oscillation occurs at the voltage across the discharge channel before it breakdown. And, the current pulse arises after the oscillation. This may have happened because of the active medium is operated at low pressure (1 mbar) since this system is not working well in low pressure condition. At this pressure, the discharge pin is difficult to breakdown, and other pins may have breakdown earlier

(D.) Inductance of the discharge circuit

The inductance of the discharge system can be obtained through the discharge voltage waveform measured at the discharge electrode. The inductance can be calculated by the following equation:

$$L = \frac{T_{1/2}^2}{\pi^2 C} \qquad \ldots\ldots \text{(Eq. 1)}$$

where $T_{1/2}$ is the half period and C is the capacitance.

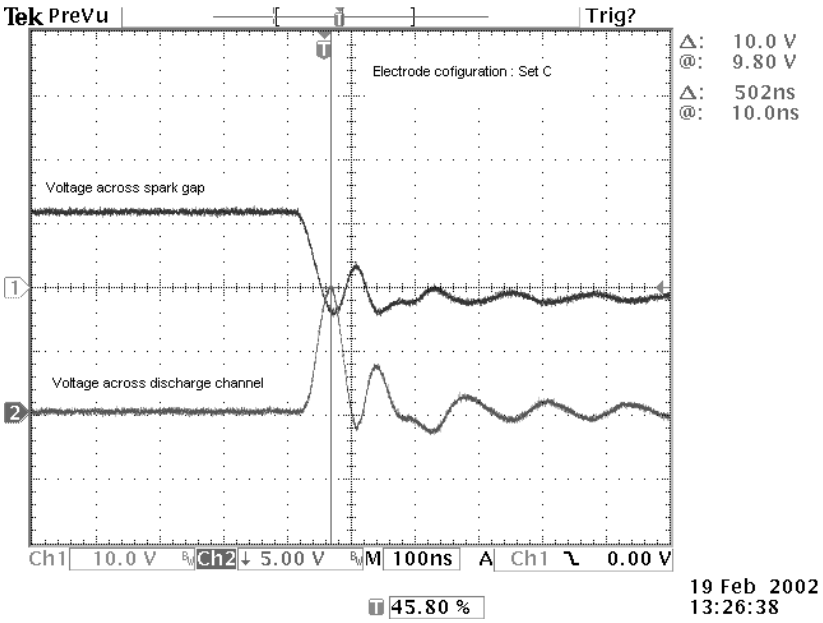

Figure 10: Discharge voltage waveform. Chn 1 indicates the voltage waveform measured across the spark gap, while Chn 2 indicates the voltage waveform measured at one of the discharge electrodes.

In Fig. 10, the $T_{1/2}$ is (40 ± 10) ns. The total peaking capacitance is 5.28 nF. Thus, the inductance of the discharge loop is calculated to be (30 ± 10) nH. The inductance of the charging loop also can be calculated using Eq. 1 as well as the inductance of the discharge loop. The inductance of the charging loop can be calculated from the voltage waveform measured across the spark gap. Referring to Fig. 6, $T_{1/2}$ is (50 ± 10) ns. The capacitance is 3.24 nF, thus gives the inductance of (70 ± 30) nH only.

CONCLUSION

This paper had detailed the discharge characteristics of the transverse arc array discharge system in two different gas mediums, i.e. nitrogen and argon. Both gases are good candidates as the investigation medium for the transverse arc array discharge. Three different electrode configurations have been investigated. In the case of electrode Set C (flat–to–flat pins), the peaking voltage obtained is the highest compared to Set A (round–to–flat pins) and Set B (round pin–to–rod). Thus, the electrode configuration of Set C, which can hold higher voltage before breakdown, is preferred. The inductance of the circuit, especially the inductance across the laser channel somehow has to be reduced by changing its transmission line geometry. The present system cannot be operated in the pressure lower than 1 mbar. For $p \leq 1$ mbar, it starts to spark. Thus, a better vacuum condition should be worked out in the future. Once the vacuum condition is good, gases like hydrogen, helium, oxygen and neon can be tested as the active medium.

One important feature of a transverse arc array discharge appropriate for Extreme Ultra Violet (EUV) and Vacuum Ultra Violet (VUV) (Hodgson, R. T., 1970) (Koehler, H. A. et. al, 1974) lasing is a short ringing period together with a sufficient high electrical energy. Such a setup may need to be scaled up the input energy to pump gases to higher state of ionization for output in VUV and XUV regions. Based on the formula of energy, $E = ½ mc^2$, the applied voltage needs to be increased instead of the capacitance. This is to ensure that higher energy can be achieved and yet create a fast and high current pulse. Therefore, a Marx generator is needed for the very high voltage requirement .

By doing so, it is hoped to achieve condition favourable to short wavelength lasers using simple electrical excitation methods.

REFERENCES

Goh, K. S. 2000. Investigations of transverse arc array laser action in nitrogen gas. *M.Sc (Applied Physics) Thesis.* University of Malaya.

Hodgson, R. T. 1970. Vacuum-ultraviolet laser action observed in the Layman bands of molecular hydrogen. *Phys. Rev. Lett.*, **25**: 494.

Koehler, H. A., Ferderber, L. J., Redhead, D. L., Ebert, P. J. Feb. 1974. VUV emission from high-pressure xenon and argon excited by high-current relativistic electron beams. *Phys. Rev. A*, **9**:768.

Ng, K. F. 2000. Optimisation of transverse arc array laser. *M.Sc (Applied Physics) Thesis.* University of Malaya.

Rocca, J. J. 1999. Table-top soft x-ray lasers. *Rev. Sci. Instrum.*, **70**: 3799.

Shipman, J. D. 1967. Traveling-wave excitation of high power gas lasers. *Appl. Phys. Lett.*, **10**: 3.